RSC Advances

COMMUNICATION

View Article Online
View Journal | View Issue



Cite this: *RSC Adv.*, 2014, **4**, 58660

# Hydrogen evolution reaction (HER) over electroless-deposited nickel nanospike arrays†

Hitoshi Ogihara,* Mizuho Fujii and Tetsuo Saji

Received 2nd October 2014
Accepted 23rd October 2014

DOI: 10.1039/c4ra11646a

www.rsc.org/advances

The hydrogen evolution reaction (HER) was carried out over Ni nanospike arrays prepared by electroless deposition. The Ni nanospike arrays showed higher HER activity than Ni plates and electrodeposited Ni because their nano-sized roughness results in a high surface area.



Hydrogen is a promising alternative energy instead of fossil fuels such as petroleum and natural gas. A feature of hydrogen fuel is its cleanliness: only water is produced in the combustion of hydrogen, which means greenhouse gases and harmful materials are not emitted. However, current hydrogen production processes mainly rely on steam reforming and partial oxidation of hydrocarbons, in which a large amount of carbon dioxide (a typical greenhouse gas) is inevitably formed as a by-product. An alternative process to produce hydrogen is water electrolysis. Electricity generated from renewable energy sources such as solar and wind power can be used to electrolyze water, and hydrogen energy produced from the water splitting reaction does not involve the emission of carbon dioxide. The hydrogen evolution reaction (HER; $2H^+ + 2e^- \rightarrow H_2$) and oxygen evolution reaction (OER; $2H_2O \rightarrow O_2 + 4H^+ + 4e^-$) are half reactions of the water splitting reaction. In water electrolysis, electrodes with a small overpotential for HER and OER can make the costs of the processes low. However, the most active electrode for HER is Pt. Hence, non-noble metal electrodes with high HER activities are being sought.[1,2]

Ni is known as an effective electrode for HER. The abundance of Ni attracts attention as an alternative electrode for HER, and the improvement of HER activity of Ni-based electrodes is an important issue to be solved. One major approach to enhance the HER activity of Ni electrodes is alloying.[3–9] Using density functional theory, Liu and Rodriguez predicted that Ni–P alloy could be an excellent catalyst for HER,[3] and recently, Popczun *et al.* demonstrated Ni–P alloy nanoparticles prepared in solution-phase showed high HER activity.[4] The other strategy is to increase electrochemically active site, which is frequently achieved by introducing nano-structure on Ni electrodes.[10–14] For example, Chen *et al.* reported that Ni nanowires that are vertically grown on substrates using anodic aluminum oxide as templates had high HER activity.[14] Such nano-structured films have been often prepared using templates, and the removal of the templates results in the formation of nano-structures.

In the present study, we focused on Ni nanospike arrays prepared by electroless deposition without templates, and firstly examined HER activity of the Ni nanospike arrays. Ni nanospike arrays were deposited onto Cu substrates using a bath ($NiCl_2 \cdot 6H_2O$: 0.05 M, $H_2NNH_2 \cdot H_2O$: 0.10 M, glycine: 0.30 M, and $H_3BO_3$: 0.50 M. pH was adjusted to 12 by adding KOH).[15] As soon as chemically-etched Cu substrates were immersed into the bath heated at 353 K, electroless deposition of Ni took place. During the electroless deposition, we could see that nitrogen gas vigorously evolved according to the following equation.[16]

$$2Ni^{2+} + N_2H_4 + 4OH^- \rightarrow 2Ni + N_2 + 4H_2O \quad (1)$$

As shown above, electroless deposition is a one-step process that does not require costly instrumentation and extreme reaction conditions.

In addition to the Ni nanospike arrays, commercially available Ni plates and electrodeposited Ni were also used as electrodes for HER. The electrodeposited Ni was prepared using a typical electrodeposition bath. Detail experimental procedure was described in the ESI.†

Fig. 1 shows SEM images of the electroless deposited Ni films. Ni crystallites were uniformly deposited over the substrates at early stage of the electroless deposition (Fig. 1(a)). From the SEM image with higher magnification (Fig. 1(b)), we can see that the electroless deposited Ni had spiky structure. The size of the nanospikes was ranged from several tens to several hundreds nanometres, and they tend to grow vertically.

*Department of Chemistry & Materials Science, Tokyo Institute of Technology, 2-12-1, Ookayama, Meguro-ku, Tokyo 152-8552, Japan. E-mail: ogihara@cms.titech.ac.jp; Fax: +81-3-5734-2624; Tel: +81-3-5734-2624*

† Electronic supplementary information (ESI) available: Experimental procedure; photographs, XRD patterns, SEM images, EDS analyses, CV, EASA, and LSV of the electrodes. See DOI: 10.1039/c4ra11646a

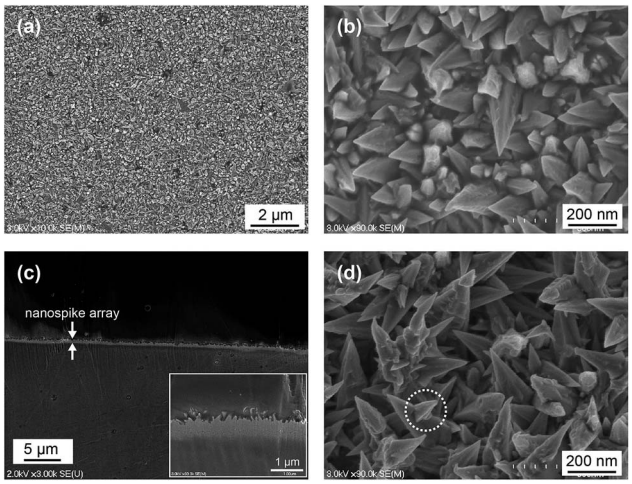


Fig. 1 Surface and cross-sectional FE-SEM images of Ni nanospike arrays. Electroless deposition time: (a–c) 5 and (d) 60 min.

So far, it is reported that spiky Ni nanoparticles are formed by using hydrazine as a reductant,[16–20] and such spiky structure does not form when using other reductants (*e.g.*, $NaBH_4$ and $NaH_2PO_2$).[4,9,21] Since we also used hydrazine as the reductant for $Ni^{2+}$, the deposition of spiky Ni on the substrates resulted in the formation of nanospike arrays. Probably, hydrazine adsorbs on a specific crystal plane of Ni, which cause anisotropic growth to form nanospike shape. The cross-sectional SEM image (Fig. 1(c)) shows that electroless deposition of Ni took place uniformly over the substrate. The nanospike structure can be observed after 60 min of electroless deposition (Fig. 3(d)). It seems that Ni nanospikes grow from on the surface of other nanospikes (the white circle in Fig. 3(d)). The appearance of the Ni nanospike arrays was black (Fig. S1†), which means visible light scattered due to the roughness in the nanospike arrays. On the contrary, electrodeposited Ni has bright appearance (Fig. S1†) and flat surface (Fig. S2†), indicating electroless deposition is useful for the preparation of characteristic nanostructured Ni.

Fig. 2 shows XRD patterns of a Ni plate, electrodeposited Ni, and the Ni nanospike arrays. The XRD patterns indicate only Ni metal phase was formed in the electrodeposited Ni and the Ni nanospike arrays. The preferred orientation of the nanospike arrays was different from the corresponding one of the Ni plate and the electrodeposited Ni; while Ni(111) was preferred in the nanospike arrays, Ni(200) was preferred in the Ni plate and the electrodeposited Ni. Similar preferred orientations were also observed in spiky Ni nanoparticles prepared by electroless deposition;[18,20] therefore, the preferred orientation of the Ni nanospike arrays shown in Fig. 2 would be the feature of anisotropic nanostructure formed *via* electroless deposition.

Comparing XRD patterns of the Ni nanospike arrays prepared at different reaction time, we can see that when the electroless deposition time was longer, the diffraction lines due to Ni and Cu (substrate) became stronger and weaker respectively, which means Ni grows constantly during the electroless deposition. The XRD patterns (c–e) show Ni(111) was dominant regardless of the electroless deposition time, *i.e.*, the preferred orientation of the Ni nanospikes did not depend on the reaction time. It is considered that the growth of nanospike arrays proceeds in the same way during the electroless deposition.

HER activities of the Ni electrodes were evaluated from linear sweep voltammetry in 1 M KOH using an electrochemical workstation (CV-50W, BAS, Inc.). Fig. 3(a) shows HER over the Ni nanospike array, the Ni plate, and the electrodeposited Ni electrodes. Fig. 3(a) clearly shows that HER activities of the Ni plate and electrodeposited Ni were almost the same, while the nanospike array has much higher HER activity than them. When the onset potential for HER was defined as the potential where current density reached 1 mA $cm^{-2}$, the onset potentials for the Ni plate, the electrodeposited Ni, and the Ni nanospike array are −1.27, −1.23, and −1.20 V, respectively. The result also supports the effectiveness of the Ni nanoneedle array for HER. Fig. 3(b) shows HER over Ni nanospike arrays prepared at

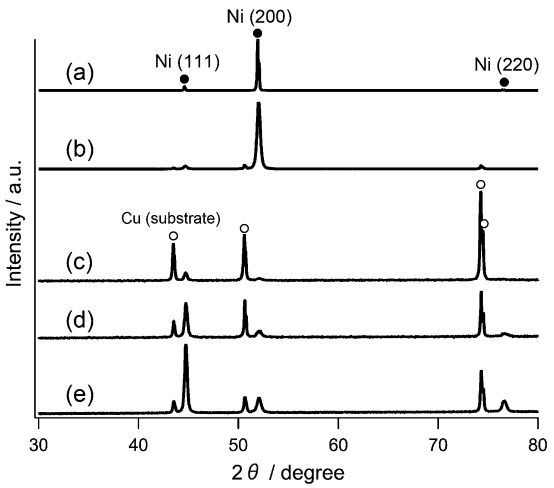


Fig. 2 XRD patterns of (a) Ni plate, (b) electrodeposited Ni, and Ni nanospike arrays prepared from electroless deposition for (c) 5, (d) 20, and (e) 60 min.

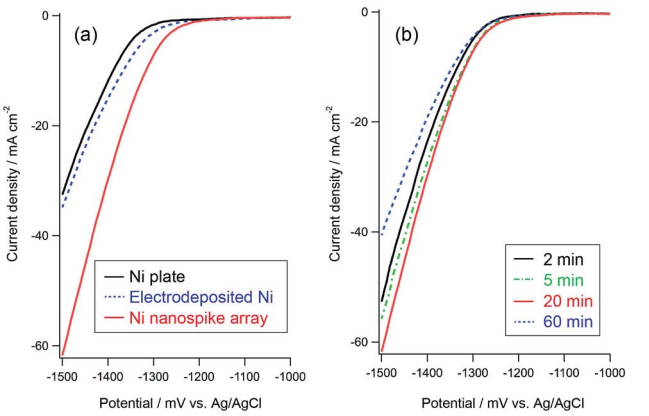


Fig. 3 LSV in 1 M KOH aqueous solution at 10 mV $s^{-1}$ of scan rate. Electrodes: (a) Ni plate, electrodeposited Ni, and Ni nanospike array; and (b) Ni nanospike arrays prepared from electroless deposition for 2, 5, 20, and 60 min.

different electroless deposition time. HER activities slightly increased as the electroless deposition time was prolonged from 2 min to 20 min, and the electrode prepared from electroless deposition for 60 min showed the lowest HER activity. From Fig. 3, we can conclude that the Ni nanospikes arrays are effective electrodes for HER and their HER activities depends on electroless deposition time. Note that the properties of the Ni nanospike arrays such as crystalline structure, chemical composition, and surface morphology were not changed after HER (Fig. S3 and S4†).

To discuss the difference in the HER activities, we focused on the number of active site on the Ni electrodes. As shown in SEM images, nanospike arrays provide highly rough surface, which must increase electrochemically active surface area (EASA). EASA of Ni electrodes are measurable using electrochemical oxidation of Ni ($Ni + 2OH^- \rightarrow \alpha Ni(OH)_2 + 2e^-$) which only occurred on monolayer of Ni electrodes.[22,23] The measured surface areas should reflect the amount of electrochemically active site where electrolyte is accessible. The electrochemical analyses of the Ni electrodes provided the order of their EASA: Ni plate $\approx$ electrodeposited Ni < Ni nanospike arrays (Fig. S5 and Table S1†). We considered that the high EASA of Ni nanospike arrays is caused by their roughness. The high EASA of the nanospike arrays must lead to superior HER activity.

As for electroless deposition time, the surface area became larger as the electroless deposition time prolonged (Fig. S5 and Table S1†). The growth of nanospike structure would contribute to enlarge their surface area. However, HER activities of the nanospike arrays are not simply related to their surface areas. From 2 min to 20 min of electroless deposition, both HER activities and surface areas of the nanospike arrays increased, but HER activity of the Ni nanospike array (60 min) drastically decreased despite the fact that the nanospike (60 min) has the largest surface area. The discrepancy would be explained by the formation of hydrogen gas in porous structure of the nanospike arrays. The formed hydrogen gas could be trapped in nanoporous structure; as a result, such part cannot contact with electrolyte and the trapped gas hinder ionic transportation.[24] For example, Chen *et al.* prepared Ni nanowires using anodic aluminum oxide as template and demonstrated Ni nanowires showed higher HER activities than planar Ni plate because of large surface area of the Ni nanowires, but HER activities of the Ni nanowires were not proportional to their surface areas because of the above reasons.[14] We considered that the similar phenomena would be observed in the Ni nanospikes arrays. Nanostructure of the nanospike arrays develops as increasing electroless deposition time, and EASA also increased. However, hydrogen formed in the nanostructure tends to remain, and interferes in HER. This is the reason why the nanospike array prepared at 60 min of electroless deposition showed low HER activity despite its high surface area. Finally, electrode performance per EASA was compared (Fig. S6†). It is considered that intrinsic activities of the Ni electrodes used in this work are almost the same, because the electrode performance per EASA was similar in the Ni plate, the electrodeposited Ni, and the Ni nanospike array (2 and 5 min). The drastic decrease in HER activity per EASA with electroless deposition time backs up the assumption that hydrogen trapped in nanospike hindered HER. Although high EASA of the Ni nanospike due to the roughness promotes HER activity, the roughness also degrade the electrode performance due to trapping hydrogen. Therefore, it could be concluded that moderate roughness where the formed gas is easily removed is suitable for HER.

## Conclusions

Ni nanospike arrays were synthesized *via* electroless deposition. The nanospike arrays showed higher HER activity than commercially-available Ni plate and electrodeposited Ni. The high HER activity is ascribed to their characteristic nanostructure; the nanospikes provide high roughness, which results in increasing EASA. However, formed hydrogen gas tended to be trapped in extremely-high roughness. Thus, electroless deposition time should be controlled to form moderate roughness. Electroless deposition has an advantage in the preparation procedure: just immersing a substrate in a bath for a few tens minutes forms an active electrode. We believe that the electroless deposited nanospike array contributes to the design of novel electrode catalytic system.

## Acknowledgements

The authors thank Mr J. Koki (Center for Advanced Materials Analysis, Tokyo Institute of Technology) for measuring FE-SEM images.

## Notes and references

1 J. Yang and H. S. Shin, *J. Mater. Chem. A*, 2014, **2**, 5979.
2 Y. Yan, B. Y. Xia, Z. Xu and X. Wang, *ACS Catal.*, 2014, **4**, 1693.
3 P. Liu and J. A. Rodriguez, *J. Am. Chem. Soc.*, 2005, **127**, 14871.
4 E. J. Popczun, J. R. McKone, C. G. Read, A. J. Biacchi, A. M. Wiltrout, N. S. Lewis and R. E. Schaak, *J. Am. Chem. Soc.*, 2013, **135**, 9267.
5 J. R. McKone, B. F. Sadtler, C. A. Werlang, N. S. Lewis and H. B. Gray, *ACS Catal.*, 2013, **3**, 166.
6 W.-F. Chen, K. Sasaki, C. Ma, A. I. Frenkel, N. Marinkovic, J. T. Muckerman, Y. Zhu and R. R. Adzic, *Angew. Chem., Int. Ed.*, 2012, **51**, 6131.
7 Z. D. Wei, A. Z. Yan, Y. C. Feng, L. Li, C. X. Sun, Z. G. Shao and P. K. Shen, *Electrochem. Commun.*, 2007, **9**, 2709.
8 S. Martinez, M. Metikoš-Huković and L. Valek, *J. Mol. Catal. A: Chem.*, 2006, **245**, 114.
9 I. Paseka, *Electrochim. Acta*, 1995, **40**, 1633.
10 I. Herraiz-Cardona, E. Ortega, L. Vázquez-Gomez and V. Pérez-Herranz, *Int. J. Hydrogen Energy*, 2012, **37**, 2147.
11 Y.-J. Huang, C.-H. Lai, P.-W. Wu and L.-Y. Chen, *J. Electrochem. Soc.*, 2010, **157**, 18.
12 Y. Yi, J. K. Lee, H. J. Lee, S. Uhm, S. C. Nam and J. Lee, *Electrochem. Commun.*, 2009, **11**, 2121.
13 A. Kellenberger, N. Vaszilcsin, W. Brandl and N. Duteanu, *Int. J. Hydrogen Energy*, 2007, **32**, 3258.

 

14 P.-C. Chen, Y.-M. Chang, P.-W. Wu and Y.-F. Chiu, *Int. J. Hydrogen Energy*, 2009, **34**, 6596.
15 K. Tashiro, T. Watanabe, H. Inaba and H. Honma, *J. Surf. Finish. Soc. Jpn.*, 2000, **51**, 606.
16 L. Bai, F. Yuan and Q. Tang, *Mater. Lett.*, 2008, **62**, 2267.
17 S. Yagi, T. Koyanagi, H. Nakanishi, T. Ichitsubo and E. Matsubara, *J. Electrochem. Soc.*, 2008, **155**, D583.
18 C. Jiang, G. Zou, W. Zhang, W. Yu and Y. Qian, *Mater. Lett.*, 2006, **60**, 2319.
19 S. L. Cheng and H. C. Peng, *J. Electrochem. Soc.*, 2010, **157**, D81.
20 C. F. Goh, H. Yu, S. S. Yong, S. G. Mhaisalkar, F. Y. C. Boey and P. S. Teo, *Mater. Sci. Eng., B*, 2005, **117**, 153.
21 H. Ogihara, T. Katayama and T. Saji, *J. Mater. Chem.*, 2011, **21**, 14890.
22 S. A. S. Machado and L. A. Avaca, *Electrochim. Acta*, 1994, **39**, 1385.
23 S. H. Ahn, S. J. Hwang, S. J. Yoo, I. Choi, H.-J. Kim, J. H. Jang, S. W. Nam, T.-H. Lim, T. Lim, S.-K. Kim and J. J. Kim, *J. Mater. Chem.*, 2012, **22**, 15153.
24 S. H. Ahn, I. Choi, H.-Y. Park, S. J. Hwang, S. J. Yoo, E. Cho, H.-J. Kim, D. Henkensmeier, S. W. Nam, S.-K. Kim and J. H. Jang, *Chem. Commun.*, 2013, **49**, 9323.